Quantum harmonic oscillators with nonlinear effective masses in the weak density approximation

Physica Scripta

PAPER

Quantum harmonic oscillators with nonlinear effective masses in the weak density approximation

Jen-Hsu Chang[1], **Chun-Yan Lin**[2,3] **and Ray-Kuang Lee**[3,4,5]

[1] Graduate School of National Defense, National Defense University, Taoyuan city 335, Taiwan
[2] National Synchrotron Radiation Research Center, Hsinchu 30016, Taiwan
[3] Institute of Photonics Technologies, National Tsing Hua University, Hsinchu 30013, Taiwan
[4] Department of Physics, National Tsing Hua University, Hsinchu 30013, Taiwan
[5] Physics Division, National Center for Theoretical Sciences, Taipei 10617, Taiwan

E-mail: rklee@ee.nthu.edu.tw

Keywords: quantum, harmonic, oscillators, nonlinear, effective

OPEN ACCESS

RECEIVED
22 September 2021

REVISED
5 January 2022

ACCEPTED FOR PUBLICATION
12 January 2022

PUBLISHED
20 January 2022

Abstract

We study the eigen-energy and eigen-function of a quantum particle acquiring the probability density-dependent effective mass (DDEM) in harmonic oscillators. Instead of discrete eigen-energies, continuous energy spectra are revealed due to the introduction of a nonlinear effective mass. Analytically, we map this problem into an infinite discrete dynamical system and obtain the stationary solutions in the weak density approximation, along with the proof on the monotonicity in the perturbed eigen-energies. Numerical results not only give agreement to the asymptotic solutions stemmed from the expansion of Hermite-Gaussian functions, but also unveil a family of peakon-like solutions without linear counterparts. As nonlinear Schrödinger wave equation has served as an important model equation in various sub-fields in physics, our proposed generalized quantum harmonic oscillator opens an unexplored area for quantum particles with nonlinear effective masses.

1. Introduction

Quantum harmonic oscillator is the most important model system in quantum mechanics, which remarkably exhibits an exact, analytical solution with discrete (quantized) eigen-energies compared to the predictions of classical counterparts [1]. Instead with a given mass, m_0, when particles (electrons or holes) move inside a periodic potential or interact with other identical particles, their motions differ from those in a vacuum, resulting in an *effective mass* [2]. With an effective mass, denoted as m^*, the corresponding Schrödinger equation for a quantum particle in a one-dimensional harmonic oscillator, characterized by the spring constant k, has the form:

$$i\hbar\frac{\partial}{\partial t}\Psi(x,\,t)=\frac{-\hbar^2}{2m^*(x)}\frac{\partial^2}{\partial x^2}\Psi+\frac{k}{2}x^2\Psi. \tag{1}$$

Here $\Psi(x, t)$ is the probability amplitude function projected in the spatial coordinate. In particular, with a nonuniform composition in potential or particle distributions, a position-dependent effective mass (PDEM) Schrödinger equation has gained much interest for its applications from semiconductors to quantum fluids [3–7]. Recently, a PDEM Schrödinger equation exhibiting a similar position-dependence for both the potential and mass was exactly solved [8]. Moreover, by taking the one-site mass in the Haldane model realized in the optical lattices, one can have similar nonlinear masses, depending on the local intensity, in the nonlinear coupled waveguide arrays for the studies on the optical isolation with nonlinear topological photonics [9].

On the other hand, it is noteworthy that equation (1) is lack of Galilean invariance, but the position-dependent effective mass Hamiltonian is by no means unique [3]. Although it is worth to construct a consistent model equation to Galilean invariance with probability density dependent effective mass, with the correspondence between Schrödinger equation and the paraxial wave equation, similar concept of position-dependent effects is also studied in the dispersion management optical fiber link [10]. Moreover, in addition to

position-dependence, chromatic dispersion may also have intensity-dependent dispersion (IDD) in the optical domains [11, 12]. IDD, or in general the nonlinear corrections to the chromatic dispersion as a function of the wave intensity, has arisen in a variety of wave phenomena, such as shallow water waves [13, 14], acoustic waves in micro-inhomogeneous media [15], ultrafast coherent pulses in quantum well waveguide structures [16], the saturation of atomic-level population [17], electromagnetically-induced transparency in a chain-Λ configuration [18], or nonlocal nonlinearity mediated by dipole-dipole interactions [19]. Inspired by IDD, in this work, we consider a quantum particle acquiring an probability density-dependent effective mass (DDEM), i.e., $m^*(|\Psi|^2)$, in a harmonic potential described by the following generalized Schrödinger equation:

$$i\hbar\frac{\partial}{\partial t}\Psi(x,\,t) = \frac{-\hbar^2}{2m_0}(1 + b|\Psi|^2)\frac{\partial^2}{\partial x^2}\Psi + \frac{k}{2}x^2\Psi. \tag{2}$$

Here, the DDEM is approximated in the weak density condition by assuming $b|\Psi|^2 < 1$. Then, we have $[m^*(|\Psi|^2)]^{-1} \equiv [m_0(1 - b\,|\Psi|^2)]^{-1} \approx [m_0]^{-1}(1 + b\,|\Psi|^2)$, with the parameter b denoting the contribution from the nonlinear effective mass term. As one can see, when the nonlinear effective mass term is zero, i.e., $b = 0$, equation (2) is reduced to the well-known scenario for a quantum particle in a parabolic potential. Besides, optical waves IDD in the Gradient-index (GRIN) lenses [20] also share the same model equation described in equation (2) when we consider wave propagation along the z-coordinate (by replacing t by z), along with a confined transverse dimension denoted by x.

When $k = 0$, even though an approximated solution with a non-physical peak value 10^{12} was illustrated in Ref. [11] for $b < 0$, it is proved rigorously that localized solitons exist only for $b > 0$ in Ref. [12]. However, with the supported harmonic potential, the scenarios can be totally different. In terms of solitons, the interplay between nonlinearity and harmonic potential has been studied for a long time [21]. Nevertheless, such localized solutions supported only with a nonlinear effective mass is never studied. Moreover, in the weak density approximation, equation (2) also shares the same mathematical form to the Salerno model in the continuum limit, which can be derived as a quantum modified discrete nonlinear Schrödinger equation, giving the time evolution of the field amplitude on the lattice [22–24]. Without considering any nonlinear potential but only with the nonlinear effective mass differs our results from the known ones.

However, when $b \neq 0$, instead of the discrete energies, continuous energy spectra are revealed due to the introduction of a nonlinear effective mass. Analytical solutions for the corresponding eigen-energy and eigen-function are derived by expanding the solutions in the weak density, i.e., $b|\Psi|^2$. Numerical solutions obtained by directly solving equation (2) give good agreement to the analytical ones obtained from the expansion of Hermite-Gaussian functions. Moreover, we unveil a family of peakon-like solutions supported by DDEM, which has no counterpart in the linear limit. Our perturbed solutions and numerical results for this generalized quantum harmonic oscillator with nonlinear effective masses opens an unexplored area for quantum particles.

The paper is organized as follows: in Session II, we introduce the quantum harmonic oscillator into this generalized Schrödinger equation with nonlinear effective mass and reduce equation (2) into an infinite dynamical system. Then, by expanding $b|\Psi|^2$ and with the help of the eigen-solutions of quantum harmonic oscillator, we study the corresponding eigen-energy with the introduction of DDEM, as a function of the parameter b. The monotonicity of the perturbed eigen-energy is also proved. In section 3, explicitly, we derive the analytical solutions of eigen-energies and the corresponding wavefunctions for the ground and second-oder excited states in the asymptotical limit. The comparison between analytical solutions and numerical results is illustrated in section 4, demonstrating good agreement on the solutions with a smooth profile, stemmed from the expansion of Hermite-Gaussian wavefunctions. A new family of peakon-like solutions with a discontinuity in its first-order derivative is also unveiled, which has no linear counterparts. Finally, we summarize this work with some perspectives in Conclusion.

2. Quantum harmonic oscillator with DDEM

Without loss of generality, in the following, we set $\hbar = 1$, $k > 0$, $m_0 = 1$ for the simplicity in tackling equation (2). Here, by lookin for the stationary solutions $\Psi(x, t) = \psi(x)e^{-iE\,t}$, we consider a family of differential equations parametrized by a continuous DDEM parameter $b \neq 0$ of the form

$$E\,\psi + \frac{1}{2}(1 + b|\psi|^2)\frac{\partial^2}{\partial x^2}\psi - \frac{k}{2}x^2\psi = 0, \tag{3}$$

where E is the corresponding eigen-energy, x denotes a real variable for the coordinate, and $\psi(x)$ is a square integrable function. This stationary Schrödinger wave equation can be seen as a generalized quantum harmonic oscillator. In addition to the stationary states considered here, this generalized nonlinear Schröoedinger equation is expected to provide an interesting platform, with non-stationary states, for further studies on the infinite dynamical system.

When $b = 0$, equation (3) becomes the well-known equation for the quantum harmonic oscillator, which supports eigen-function of the n-th order excited state in the position representation reads [25]:

$$\phi_n(x) = k^{1/8}\mu_n e^{-k^{1/2}x^2/2}H_n(k^{1/4}x), \tag{4}$$

where $\mu_n = (2^n n!\sqrt{\pi})^{-1/2}$ and $H_n(x)$ is the n-th order Hermite polynomial. The corresponding eigen-values are equal to $E_n = \sqrt{k}\,(n + \frac{1}{2})$, for any $n \in \mathbb{N}$. We are interested in finding pairs $(\psi_n,\ E_n)_b$ fulfilling equation (3) for a set $b \neq 0$.

2.1. Expanding the eigen-energies and eigen-functions with $b|\Psi|^2$

To investigate equation (2) with $b \neq 0$ (but keeping $k \neq 1$ first), we look for the solutions based on the expansion of the solution on the eigen-function $\phi_n(x)$. That is,

$$\Psi(x,\ t) = \sum_{n=0}^{\infty} B_n(t)\phi_n(x). \tag{5}$$

By plugging this expansion into equation (2), one has

$$\begin{aligned}
&i\sum_{n=0}^{\infty}\frac{dB_n(t)}{dt}\phi_n(x) + \frac{1}{2}\sum_{n=0}^{\infty}B_n(t)\frac{d^2\phi_n(x)}{dx^2} + \frac{1}{2}\sum_{p=0,q=0}^{\infty}B_p(t)\bar{B}_q(t)\phi_p(x)\phi_q(x)\left[b\sum_{n=0}^{\infty}B_n(t)\frac{d^2\phi_n(x)}{dx^2}\right]\\
&-\frac{k}{2}x^2\sum_{n=0}^{\infty}B_n(t)\phi_n(x),\\
&=i\sum_{n=0}^{\infty}\frac{dB_n(t)}{dt}\phi_n(x) - \sum_{n=0}^{\infty}E_nB_n(t)\phi_n(x)\\
&-b\sum_{n=0,p=0,q=0}^{\infty}E_nB_n(t)B_p(t)\bar{B}_q(t)\phi_n(x)\phi_p(x)\phi_q(x) + \frac{b}{2}x^2\\
&\sum_{n=0,p=0,q=0}^{\infty}B_n(t)B_p(t)\bar{B}_q(t)\phi_n(x)\phi_p(x)\phi_q(x) = 0.
\end{aligned} \tag{6}$$

Here, $\bar{B}_n$ means the complex conjugate of B_n. Then, by multiplying equation (6) with $\phi_m(x)$ and using the orthonormal property of $\phi_m(x)$, we obtain

$$b\sum_{n=0,p=0,q=0}^{\infty}\left[-E_nV_{m,n,p,q} + \frac{1}{2}W_{n,m,p,q}\right]B_n(t)B_p(t)\bar{B}_q(t) + i\frac{dB_m(t)}{dt} - E_mB_m(t) = 0, \tag{7}$$

where $V_{m,n,p,q}$, and $W_{m,n,p,q}$ are defined as:

$$\begin{aligned}
V_{m,n,p,q} &= \int_{-\infty}^{\infty}\phi_m(x)\phi_n(x)\phi_p(x)\phi_q(x)dx,\\
W_{m,n,p,q} &= \int_{-\infty}^{\infty}x^2\phi_m(x)\phi_n(x)\phi_p(x)\phi_q(x)dx.
\end{aligned}$$

As one can see from equation (7), we reduce the original partial differential equation into the infinite discrete dynamical system [26]. With the help of the recursive relation of Hermite polynomial $H_m(x)$, for example see Ref. [25], i.e., $x^2H_m(x) = m(m-1)H_{m-2}(x) + (m+1/2)H_m(x) + 1/4H_{m+2}(x)$, one can arrive at

$$\begin{aligned}
W_{m,n,p,q} = &\frac{\sqrt{m(m-1)}}{2}V_{m-2,n,p,q} + (m+1/2)V_{m,n,p,q}\\
&+\frac{\sqrt{(m+1)(m+2)}}{2}V_{m+2,n,p,q}.
\end{aligned} \tag{8}$$

Now, we look for the stationary solution in the form:

$$\Psi(x,\ t;\ E) = e^{-iE\,t}\sum_{n=0}^{\infty}B_n\phi_n(x), \tag{9}$$

with $B_n \in \mathcal{R}$. Then, for a given energy value E, one yields

$$\begin{aligned}
&b\sum_{n=0,p=0,q=0}^{\infty}(-E_nV_{m,n,p,q} + \frac{1}{2}W_{n,m,p,q})B_nB_pB_q\\
&+(E - E_m)B_m = 0.
\end{aligned} \tag{10}$$

From now on, for simplicity, we assume $k = 1$. With the help of equation (10), next, we consider the perturbation on the energy deviated from the eigen-energy E_n with the corresponding Hermite-Gaussian eigen-mode $\phi_n(x)$.

Similar to the methodology used in dealing with the nonlinear mean field in the Gross–Pitaevskii equation (GPE) [27, 28], we substitute $\psi(x;\ E) = \sqrt{P(E)}\ \phi(x)$ with $\|\phi(x)\| = 1$ into equation (3), where $P(E) = \sum_{n=0}^{\infty} B_n$ from (9), and arrive at a nonlinear eigen-energy equation:

$$E\ \phi(x) + \frac{1}{2}[1 + b\ P(E)\phi^2(x)]\phi_{xx}(x) - \frac{1}{2}x^2\phi = 0. \tag{11}$$

Once again, in equation (11), we can see that if $P(E) \to 0$, then the resulting eigen-energy $E \to E_n = n + \frac{1}{2}$. By substituting $\phi(x)$, obtained from equation (10), into equation (11), one can have the relation between E and $P(E)$ near $E_n = n + \frac{1}{2}$. In general, the perturbation approach illustrated above works for all the values of n. However, only when n is even, a neat formula can be conducted by taking the advantage of symmetric wavefunctions in $\psi(x)$. For even numbers, $2n$, the resulting eigen-energy E due to the introduction of the DDEM parameter b can be approximated as

$$\begin{aligned} E &\approx E_{2n} - b\ P(E)\left[\frac{1}{2}W_{2n,2n,2n,2n} - \left(2n + \frac{1}{2}\right)V_{2n,2n,2n,2n}\right], \\ &= E_{2n} - b\ P(E)\mu_{2n}^4\left[\frac{1}{2}\int_{-\infty}^{\infty} x^2 e^{-x^2}H_{2n}(x)^4 dx\right. \\ &\left. - \left(2n + \frac{1}{2}\right)\int_{-\infty}^{\infty} e^{-x^2}H_{2n}(x)^4 dx\right]. \end{aligned} \tag{12}$$

To compute the integrals shown in equation (12), one can utilize the Feldheim identity for the Hermite polynomials [25]:

$$H_m(x)H_n(x) = \sum_{\nu=0}^{min(m,n)} H_{m+n-2\nu}(x)2^\nu \nu!\binom{m}{\nu}\binom{n}{\nu}, \tag{13}$$

and the Titchmarsh's integral formula [29]:

$$\begin{aligned} &\int_{-\infty}^{\infty} e^{-2x^2}H_{2m}(x)H_{2n}(x)H_{2p}(x)dx \\ &= \pi^{-1}2^{m+n+p-1/2}\Gamma\left(n + p + \frac{1}{2} - m\right) \\ &\quad \times \Gamma\left(m + p + \frac{1}{2} - n\right)\Gamma\left(m + n + \frac{1}{2} - p\right), \end{aligned} \tag{14}$$

where $n + p \geqslant m$, $m + p \geqslant n$ and $m + n \geqslant p$; otherwise, the integral is zero. From equations (13) and (14), a direct calculation can yield

$$\begin{aligned} &\int_{-\infty}^{\infty} e^{-2x^2}H_{2m}(x)H_{2n}(x)^3 dx \\ &= \frac{1}{\pi}2^{m+3n-1/2}\sum_{\nu=0}^{min(2m,2n)} \nu!\binom{2m}{\nu}\binom{2n}{\nu} \\ &\quad \times \Gamma(n + \nu + 1/2 - m)\Gamma(m + n + 1/2 - \nu)^2. \end{aligned} \tag{15}$$

2.2. Monotonicity in the perturbed eigen-energy

Given $b > 0$ ($b < 0$), to ensure solutions with linear limit $\psi(x;\ E) \approx \sqrt{P(E)}\ \phi_n(x)$ to exist only if $E \geqslant E_n = n + \frac{1}{2}$ ($E \leqslant E_n = n + \frac{1}{2}$), we prove that the two integrals inside the square brackets in equation (12) is monotonic, i.e.,

$$\begin{aligned} &\frac{1}{2}\int_{-\infty}^{\infty} x^2 e^{-x^2}H_{2n}(x)^4 dx - (2n + \frac{1}{2})\int_{-\infty}^{\infty} e^{-x^2}H_{2n}(x)^4 dx \\ &< 0; \end{aligned} \tag{16}$$

or equivalently

$$W_{2n,2n,2n,2n} - (4n + 1)\,V_{2n,2n,2n,2n} < 0. \tag{17}$$

for $n \geqslant 0$. In Appendix, the proof on the monotonicity for equation (16) and equation (17) is given in details.

By using the upper and lower solution method developed in the variational calculus [27], we can further prove the existence of a positive solution (node-less state) through the corresponding Lagrangian for equation (2), i.e.,

$$\mathcal{L}[\psi(x)] = \int_{-\infty}^{\infty}\left[\left(-\frac{E}{b}+\frac{kx^2}{2b}\right)\ln|1+b|\psi|^2| + \frac{1}{2}|\psi_x|^2\right]dx,$$
$$= \int_{-\infty}^{\infty}\left[\left(\frac{kx^2}{2b}\right)\ln|1+b|\psi|^2| + \frac{1}{2}|\psi_x|^2\right]dx - E\,Q(E), \quad (18)$$
$$\equiv Z(E) - E\,Q(E), \quad (19)$$

where $Z(E) \equiv \int_{-\infty}^{\infty}\left[(\frac{kx^2}{2b})\ln|1+b|\psi|^2| + \frac{1}{2}|\psi_x|^2\right]dx$. Here, we also introduce the *probability factor* Q for this quantum harmonic oscillator with DDEM, by defining

$$Q \equiv \frac{1}{b}\int_{-\infty}^{\infty}\ln|1+b|\psi|^2|\,dx. \quad (20)$$

As the original generalized Schrödinger equation given in equation (2) preserves the U(1) symmetry, i.e., $\psi \to \exp[i\theta]\psi$, the conserved density for this model equation can be derived from Noether theorem [30]. It is marked that the local conservation law is also valid, i.e., $\partial_t[\frac{1}{b}\ln(1+b|\Psi|^2)] + \partial_x J = 0$ with $J = \frac{1}{2i}(\Psi^*\partial_x\Psi - \Psi\partial_x\Psi^*)$. It is noted that equation (20) is only applicable when $b \neq 0$. When $|b| \ll 1$, this probability factor Q can be approximated as

$$\lim_{b\ll 1} Q \approx \int_{-\infty}^{\infty}|\psi|^2\,dx, \quad (21)$$

which is reduced to the standard definition of probability for quantum wavefunctions. For $b \to 0$, the corresponding Lagrangian density given in equation (18), as well as the conserved density given in equation (20), both go to $|\psi|^2$.

These two terms, $Z(E)$ and $Q(E)$, shown in equation (19), correspond to the Lagrangian of our generalized harmonic oscillator and the conserved quantity, respectively. As the DDEM parameter $b \to 0$, the Lagrangian shown in equation (19) can be reduced to

$$\int_{-\infty}^{\infty}\left(-E\,|\psi|^2 + \frac{k}{2}x^2|\psi|^2 + \frac{1}{2}|\psi_x|^2\right)dx,$$

which is the Lagrangian for the linear equation, i.e., $-\frac{1}{2}\psi_{xx} + \frac{k}{2}x^2\psi = E\,\psi$. By following the same concept in tackling weak non-linearity [31], the perturbation based on the expansion of the Hermite-Gaussian functions to deal with the DDEM ensures that when $E \to E_n$, one has $Q(E) \to 0$.

3. Eigen-energies and eigen-functions obtained from perturbation

3.1. The ground state

Now with the analytical formula give in equation (12), we explicitly give the perturbed eigen-energy E and eigen-function $\psi_0^b(x)$ for the ground state in our generalized quantum harmonic oscillator with a given DDEM parameter b. For the ground state, we can assume that $B_0 \gg B_{2n}$, $n = 1, 2, 3, \cdots$. Then, from equation (10), one has

$$B_0^2 \approx \frac{E - E_0}{b(-\frac{1}{2}W_{0,0,0,0} + \frac{1}{2}V_{0,0,0,0})}, \quad (22)$$

and

$$B_{2n} \approx \frac{bB_0^3(-\frac{1}{2}W_{2n,0,0,0} + E_0\,V_{2n,0,0,0})}{(E - E_{2n})},$$
$$= B_0\frac{\left(E - E_0\right)\left(-\frac{1}{2}W_{2n,0,0,0} + E_0\,V_{2n,0,0,0}\right)}{\left(E - E_{2n}\right)\left(-\frac{1}{2}W_{0,0,0,0} + \frac{1}{2}V_{0,0,0,0}\right)}, \quad (23)$$

where $\Gamma_{m,n}$, $V_{m,n,p,q}$, and $W_{m,n,p,q}$ have the values:

$$W_{0,0,0,0} = \frac{1}{4\sqrt{2\pi}},$$
$$V_{0,0,0,0} = \frac{1}{\sqrt{2\pi}},$$
$$V_{2n,0,0,0} = \frac{(-1)^n}{\sqrt{\pi 2^{2n+1}(2n)!}}(2n-1)!!,$$
$$W_{2n,0,0,0} = \frac{(-1)^{n+1}}{\sqrt{\pi 2^{2n+5}(2n)!}}(2n-1)!!(2n-1),$$

for $n \geqslant 1$. Therefore, from equations (22) and (23), explicitly we have, noting that $E_0 = \frac{1}{2}$, $E_n = n + \frac{1}{2}$,

$$B_0^2 \approx \frac{8\sqrt{2\pi}}{3b}\left(E - \frac{1}{2}\right), \tag{24}$$

$$B_{2n} \approx bB_0^3 \frac{(-1)^n(\frac{1}{4}n + \frac{3}{8})(2n-1)!!}{\sqrt{\pi 2^{2n+1}(2n)!}\,(E - 2n - \frac{1}{2})}, \tag{25}$$

$$\approx \frac{1}{8} bB_0^3 \frac{(-1)^{n+1}(2n-1)!!}{\sqrt{\pi 2^{2n+1}(2n)!}}, \quad \text{as} \quad n \to \infty. \tag{26}$$

With the coefficients above, the perturbed solution of $\psi_0^b(x)$ can be conducted immediately as

$$\psi_0^b(x) \approx B_0\phi_0(x) + B_2\phi_2(x) + B_4\phi_4(x) + \cdots.$$

We notice that $\psi_0^b(x) \to \phi_0(x)$ as $E \to E_0 = \frac{1}{2}$. Again, with the orthonormality of $\phi_{2n}(x)$, in the asymptotical limit, $n \to \infty$, the probability factor Q defined in equation (20) becomes:

$$\begin{aligned} Q(E) &= \frac{1}{b}\int_{\infty}^{\infty} \ln|1 + b|\psi_0^b|^2(x)|dx, \\ &\approx \int_{-\infty}^{\infty} |\psi_0^b|^2(x)dx = B_0^2 + B_2^2 + B_4^2 + \cdots. \\ &\approx \frac{8\sqrt{2\pi}}{3b}\left(E - \frac{1}{2}\right)\left[1 + \frac{1}{9}\left(E - \frac{1}{2}\right)^2 \sum_{n=1}^{\infty} \frac{(2n)!}{(n!2^{2n})^2}\right], \end{aligned} \tag{27}$$

It is noted that the identity $(2n-1)!! = \frac{(2n)!}{2^n n!}$ is applied. Therefore, we see that $Q(E) \to 0$ as $E \to E_0 = \frac{1}{2}$. As one can see from equation (27), the probability factor $Q(E)$ is linearly proportional, in the leading order, to the eigen-energy E, but with the coefficient inversely proportional to the DDEM parameter b.

3.2. The second order excited state

In addition to the ground state with $n = 0$, in general, all the perturbed eigen-energy E_{2n}^b and eigen-function $\psi_{2n}^b(x)$ can be written explicitly. Here, we illustrate the solutions for the second order excited state, E and $\psi_2^b(x)$, by assuming $B_2 \gg B_{2n}$, $n = 0, 2, 3, \cdots$. Again, with equations (8) and (10), one can directly obtain:

$$B_2^2 \approx \frac{E - E_2}{b\left[\frac{-\sqrt{2}}{4}V_{0,2,2,2} - (\frac{5}{4} - E_2)V_{2,2,2,2} - \frac{\sqrt{3}}{2}V_{4,2,2,2}\right]}, \tag{28}$$

and

$$B_{2n} \approx \frac{bB_2^3(-\frac{1}{2}W_{2n,2,2,2} + E_2 V_{2n,2,2,2})}{(E - E_{2n})}, \tag{29}$$

with

$$V_{2n,2,2,2} = \frac{(-1)^{n-3}(2n-1)!!(8n^3 - 60n^2 + 94n - 1)}{\sqrt{\pi 2^{2n+10}(2n)!}}. \tag{30}$$

As a result, we we have

$$B_2^2 \approx \frac{256\sqrt{2\pi}}{327b}(E - E_2), \tag{31}$$

and

$$\begin{aligned} B_{2n}^2 &\approx \frac{b^2B_2^6(2n)!(16n^4 - 112n^3 + 32n^2 + 476n + 23)^2}{2^{4n+16}\pi(n!)^2(E - E_{2n})^2}, \\ &\approx b^2B_2^6\frac{(2n)!n^6}{2^{4n+10}\pi(n!)^2}, \qquad \text{as} \quad n \to \infty. \end{aligned} \tag{32}$$

Then, the perturbation of $\psi_2^b(x)$ can be constructed by collecting the coefficients above, i.e., $\psi_2^b(x) \approx B_2\phi_2(x) + B_4\phi_4(x) + B_6\phi_6(x) + \cdots$. It is noted that here, the expansion starts from $n = 2$ as $B_0 = 0$. Again, we have $\psi_2^b(x) \to \phi_2(x)$ as $E \to E_2 = \frac{5}{2}$. Moreover, thee resulting probability factor $Q(E)$ in the asymptotical limit, $n \to \infty$ has the form:

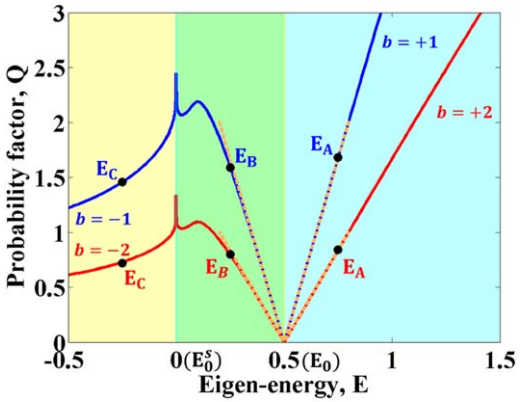

Figure 1. The probability factor $Q(E)$ defined in equation (20) for the ground state in quantum harmonic oscillator with DDEM, as a function of eigen-energy E. Here, the DDEM parameter b is set as ± 1 and ± 2, depicted in Blue- and Red-colors, respectively. The ground state energy in the linear limit, $b = 0$, is marked as $E_0 = 0.5$. Analytical solutions based on the perturbation theory given in equation (27) are also depicted in the dashed-curves, which illustrate good agreement to the numerical solutions near E_0. Moreover, three different regions for the supported eigen-functions are identified for those with a smooth profile stemmed from the expansion of Hermite-Gaussian wavefunctions (in Blue- and Green-colored backgrounds for $b > 0$ and $b < 0$, respectively); and with a peakon-like profile having a singularity in its first-order derivative (in Yellow-color background).

$$\begin{aligned} Q(E) &= \frac{1}{b}\int_{-\infty}^{\infty} \ln|1 + b|\psi_2^b(x)|^2|dx, \\ &\approx \int_{-\infty}^{\infty} |\psi_2^b|^2(x)dx = B_2^2 + B_4^2 + B_6^2 + \cdots. \\ &\approx \frac{512\sqrt{2\pi}}{435b}\left(E - \frac{5}{2}\right) \\ &\quad \times \left[1 + \frac{2 \times 512^2}{435^2}\left(E - \frac{5}{2}\right)^2 \sum_{n=1}^{\infty} \frac{(2n)!n^6}{(n!2^{2n+5})^2}\right]. \end{aligned} \tag{33}$$

Here, again, we see that $Q(E) \to 0$ as $E \to E_2 = \frac{5}{2}$.

In addition to the ground and second order excited states, for all the even number of n, the perturbed eigen-energy E_{2n}^b and eigen-function $\psi_{2n}^b(x)$, as well as the corresponding probability factor $Q(E_{2n}^b)$, can be derived explicitly, with the help of equations (10), (12) and (20), respectively. As for the odd number of n, equations (10) and (11) provide the required conditions to have the eigen-energy and eigen-function with the introduction of the DDEM parameter b.

4. Numerical results by direct simulations

4.1. The ground state

In order to verify the validity of our analytical solutions obtained by the expansion, we also perform the numerical calculations for equation (3) directly without applying any approximation. Here, the eigen-values/eigen-functions are generated by substituting the eigen-function iteratively until a convergent eigen-value is reached. Moreover, the linear stability method is applied for the found eigen-function. All the found eigen-functions are stable due to the harmonic potential. To maintain some level of formal rigor and mathematical correctness, we shall talk about finding solutions of differential equations [32]. To find the solutions of the eigen-value problem with the nonlinear term, we connect with a quantum harmonic oscillator by solving equation (3) with Fourier spectral method. Using the matrix elements, we diagonalize the matrix numerically and perform the iteration to ensure that the truncated Fourier basis makes the eigen-value convergent. For low energy states, already the smallest basis of 512 elements gives more than sufficient accuracy.

In figure 1, we show the corresponding lowest eigen-mode of the generalized quantum harmonic oscillator described in equation (3), in the plot of probability factor versus eigen-energy Q-E. Starting from $E_0 = 0.5$, i.e., the eigen-energy of ground state in the standard quantum harmonic oscillator with $b = 0$; however, the eigen-energy is not a discrete value, but a continuous function due to the introduction of DDEM, i.e., $b \neq 0$. Here, the initial guess solution has a single-hump profile, i.e., a Gaussian function stemmed from the zero-th order $H_n(x)$. With a positive value of b, such as $b = 1$ and $b = 2$, shown in Blue- and Red-colored curves in figure 1, the corresponding probability factor $Q(E)$ presents an almost linear function of the eigen-energy E. Now, all the eigen-energy E_0^b are larger than that of E_0. Compared to the analytical formula of $Q(E_0^b)$ obtained in

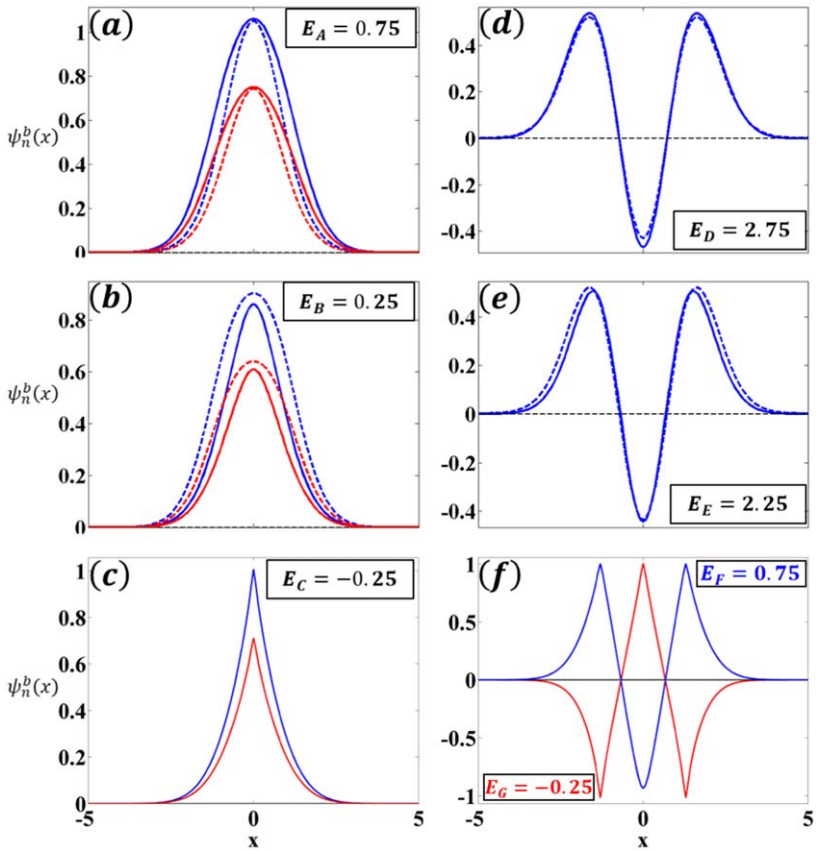

Figure 2. The wavefunction for (a)–(c) the ground state $\psi_0^b(x)$ and (d)–(f) the second order excited state $\psi_2^b(x)$ of the quantum harmonic oscillator with DDEM $b = \pm 1$ and $b = \pm 2$, shown in Blue- and Red-colored curves, respectively, i.e., corresponding to the markers (E_A, E_B, E_C) and (E_D, E_E, E_F and E_G) labelled in figures 1 and 3, respectively. The analytical results based on the perturbation theory are depicted in the dashed-curves, for $\psi_0^b(x)$ and $\psi_2^b(x)$, accordingly. Here, the selected eigen-energies E are chosen to represent the typical profile of wavefunctions in three different regions: (a), (d) a smooth profile with $b > 0$; (b), (f) a smooth profile with $b < 0$, and (c), (f) a peakon-like solution with $b < 0$.

equation (27), the dashed-curves give agreement to the numerical ones, not only on the slope of Q-E curves but also on the inversely proportional dependence on b.

Moreover, the corresponding wavefunction $\psi_0^b(x)$ is depicted in figure 2(a), which shares a similar Gaussian profile with that in the linear case $b = 0$. For example, at the marked eigen-energy $E_A = 0.75$, the eigen-functions $\psi_0^b(x)$ have similar Gaussian shapes both for $b = 1$ and $b = 2$. But the resulting amplitude, as well as the width, is smaller with a larger value in the DDEM parameter, such as $b = 2$. The analytical solutions obtained by perturbed theory, depicted in dashed-curves in figure 2(a), also reflect this similarity.

However, when b is negative, there are two distinct regions in this Q-E curve, illustrated in the Green- and Yellow-colored backgrounds in figure 1. For the Green-colored region, the corresponding eigen-energy is smaller than $E_0 = 0.5$, but remains positive, i.e., $0 < E_0^b < E_0$. The probability factor $Q(E_0^b)$ is also linearly proportional to the eigen-energy E, as predicted by our analytical formula in equation (27). But, now the slope of Q-E curve changes its sign, as the $b < 0$. The resulting wavefunction $\psi_0^b(x)$, as shown in figure 2(b) for the marked eigen-energy $E_B = 0.25$, still has a smooth profile. However, the corresponding width of wavefunction shrinks when $E \to 0$. As a result, a singularity emerges at $E_0^s = 0$ for the ground state, in which no well-defined localized wavefunction can be supported. The singularity comes from the divergence of $Q(E)$ near $1 + b|\psi|^2 = 0$. Moreover, as one can see, our theoretical formula also breaks down when E approaches this singularity.

Unexpectedly, single-hump solutions can be supported even when $E < E_0^s = 0$, as shown in the Yellow-colored region. As shown in figure 2(c) for the marked eigen-energy $E_C = -0.25$, instead of a smooth profile stemmed from the Gauss wavefunction, the resulting wavefunction of this family of peakon-like solutions has a discontinuity in its first-order derivative, similar to the peakon solution in the form of $\exp(-|x|)$. Such peakon-like solutions are also already found in the IDD setting for optical waves, even without the introduction of harmonic oscillators [11, 12]. As our perturbation theory starts from the eigen-basis of Hermite-Gaussian functions, it is not applicable to this family of peak-like solutions.

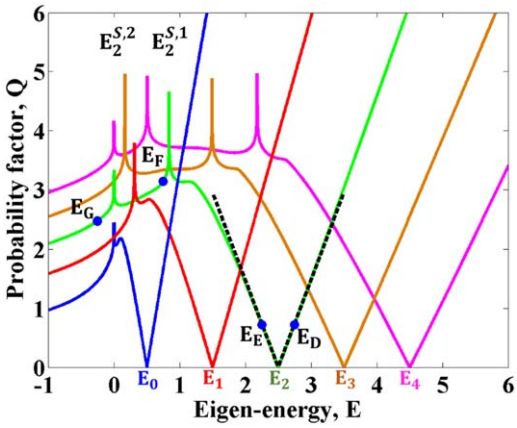

Figure 3. The probability factor versus eigen-energy curve, Q-E, for the excited states in a quantum harmonic oscillator with DDEM. Here, the DDEM parameter b is set as ± 1. The solution family with the same number of humps in the eigen-functions $\psi_n^b(x)$ are depicted in the same colors, with the labelled starting eigen-energies E_n, for $n = 0, 1, 2, 3, 4$. Analytical solutions based on the perturbation theory given in equation (33) are also depicted in the Black dashed-curves, which illustrate good agreement to the numerical solutions near $E_2 = 2.5$.

4.2. The excited states

In addition to the ground state, the founded second order excited states, both numerically and analytically, are also depicted in figure 2(d)–(f). Again, we also have three different regions in charactering the wavefunction profiles. Smooth profiles with the DDEM $b > 0$ and $b < 0$ are shown in (d) and (e) for the marked eigen-energies $E_D = 2.75 > E_2 = 2.5$ and $E_E = 2.25 < E_2$ in figure 3, respectively. As shown in figures 2(d) and (e), the two solutions, $\psi_2^b(x)$ have three humps in their profiles and share the similar profile as the 2nd order Hermite-Gaussian function. By comparing the solid- and dashed-curves, corresponding to our numerical results and analytical solutions, respectively, one can see nearly perfect agreement for the solutions around the eigen-energy E_2.

Moreover, a discontinuous profile emerges when $b < 0$ and $E < E_2^{s,1}$, where the singularity happens. Unlike the Q-E curves for the ground state, there exist two singularities, denoted as $E_2^{s,1} \approx 0.8398$ and $E_2^{s,2} = 0$. When the eigen-energy is smaller than the value at the first singularity $E_2^{s,1}$ but larger than the value at the second singularity $E_2^{s,2}$, for example $E_F = 0.75$, the peakon-like solution illustrated in Blue-color in figure 2(f), has a profile of $\exp(-|x|)$ in two of the humps in the sidebands. It is noted that the profile in the central hump remains a smooth function. Nevertheless, when the eigen-energy is smaller than the value at the second singularity $E_2^{s,2}$, for example $E_G = -0.25$, the corresponding eigen-function has discontinuities in all the three humps, as depicted in Red-color in figure 3(f).

In figure 3, we plot all the founded eigen-energies, up to $n = 4$, by depicting the solution family with the same number of humps in the eigen-functions $\psi_n^b(x)$ in the same colors. One can see clearly that, all the Q-E curves start from the eigen-energies $E_n = n + \frac{1}{2}$ of a standard quantum harmonic oscillator, i.e., $b = 0$. Around these energy values, E_n, our perturbation theory works perfectly, giving the linear dependence of $Q(E)$ on the eigen-energy, along with the inversely proportional relation to the DDEM parameter b. In particular, as depicted in the dashed-curves, it can be seen clearly that our analytical solutions given in equation (33) illustrate good agreement to the numerical solutions near $E_2 = 2.5$.

However, when b turns negative and the supported eigen-energy E_n^b is away from the starting energy value E_n, one more singularities appear at certain value(s) of E_n^s. The number of singularity depends on the critical points of the Hermite polynomial due to the divergence of $Q(E)$ near $1 + b|\psi|^2 = 0$. Considering the symmetry of Hermite polynomial, i.e., $H_n(x) = \pm H_n(-x)$, as one can see from figure 3, the number of singularities for $Q(E_{2n}^b)$ and $Q(E_{2n+1}^b)$ is the same, i.e., equal to $n + 1$.

Before Conclusion, we remark the stability of the founded eigen-solutions of our generalized quantum harmonic oscillator with a probability density-dependent effective mass (DDEM). As confined by the external harmonic oscillator, all the found eigen-solutions are stable numerically. The validity of our perturbation theory is limited to the eigen-energy around the known one $E_{2n} = 2n + \frac{1}{2}$. It is expected that our analytical formula breaks down when E_n^b approaches E_n^s. As for the possible bifurcation maps, how to develop an analytical method to find the solutions for these peakon-like solutions, as well as around the singularities, is a challenge, which goes beyond the scope of the current work but deserves further studies.

5. Conclusion

By introduction a probability density-dependent effective mass (DDEM) for a quantum particle in harmonic oscillators, we propose a generalized Schrödinger equation to embrace the nonlinear effective mass. With the help of orthonormal property of Hermite-Gaussian functions, we reduce this partial differential equation into an infinite discrete dynamical system and find the corresponding stationary solution by expanding $b|\Psi|^2$. The monotonicity of perturbed solutions is also approved rigorously. The resulting eigen-energy spectra is no longer discretized, but continuous due to the introduction of a nonlinear effective mass. With the comparison to numerical results obtained by direct simulations, the validity of our analytical formula in the asymptotic limit, in terms of the probability factor as a function of the eigen-energy, $Q(E)$, can be easily verified, in particular for the solutions stemmed from the expansion of Hermite-Gaussian functions. However, the nonlinear effective mass also introduces a new family of peakon-like solutions with a discontinuity in their first-order derivative, which definitely deserves further studies.

It is noted that what we illustrated in this work is based on tackling equation (2), under the weak density approximation. It is also possible to go beyond the weak density approximation by directly studying equation (1). However, according to quantum mechanics, the effective mass $m^*(x)$ does not commute with the momentum $-i\hbar\partial_x$. Instead of $1/[2m^*(x)](-i\hbar\,\partial_x)^2$, the product $(-i\hbar\partial x)1/[2m^*(x)](-i\hbar\partial_x)$ should be taken into account when the quantum particle is considered. It has been well studied with the nonlinear Schrödinger wave equation, or the Gross–Pitaevskii equation in general, where the nonlinear terms come from Kerr-effect, or the mean-field interaction. With the eigen-energy and eigen-function illustrated in this work, our proposed generalized quantum harmonic oscillator opens an unexplored area for quantum particles with nonlinear effective masses. A number of promising applications and directions for further exploration may be identified when particles accessing nonlinear correction to their effective mass. Similar models related to our proposed generalized quantum harmonic oscillators, but in more complicated settings involve off-resonant self-induced transparency (SIT) solitons [33, 34] spatially-periodic refractivity doped with two-level systems (TLS) [35, 36], electromagnetically-induced transparency (EIT) via resonant dipole-dipole interactions [37, 38], and the continuum limit of the Salerno model [22–24].

Acknowledgments

This work is partially supported by the Ministry of Science and Technology of Taiwan under Grant No.: 105-2628-M-007-003-MY4, 108-2115-M-606-001, 108-2923-M-007-001-MY3, and 109-2112-M-007-019-MY3, Office of Naval Research Global, US Army Research Office (ARO), and Center for Quantum Technology, Taiwan.

Data availability statement

All data that support the findings of this study are included within the article (and any supplementary files).

Appendix

Here, we give the details to prove the inequality shown in equations (16) and (17).

First of all, from equation (8), one can see that

$$\begin{aligned}
&W_{2n,2n,2n,2n} - (4n+1)V_{2n,2n,2n,2n}\\
&= \frac{\sqrt{2n(2n-1)}}{2}V_{2n-2,2n,2n,2n} - (2n+1/2)V_{2n,2n,2n,2n} + \frac{\sqrt{(2n+1)(2n+2)}}{2}V_{2n+2,2n,2n,2n},\\
&< nV_{2n-2,2n,2n,2n} - (2n+1/2)V_{2n,2n,2n,2n} + (n+1)V_{2n+2,2n,2n,2n},\\
&= n(V_{2n-2,2n,2n,2n} - V_{2n,2n,2n,2n}) + n(V_{2n+2,2n,2n,2n} - V_{2n,2n,2n,2n}) + (V_{2n+2,2n,2n,2n} - \frac{1}{2}V_{2n,2n,2n,2n}). \qquad \text{(A1)}
\end{aligned}$$

Then, with the formula

$$\Gamma(h+\frac{1}{2}) = \binom{h+\frac{1}{2}}{h}h!\sqrt{\pi} = \frac{(2h-1)!!}{2^h h!}h!\sqrt{\pi}, \qquad \text{(A2)}$$

one can have

$$V_{2n,2n,2n,2n} = \frac{1}{\sqrt{2\pi}}\sum_{\nu=0}^{2n}\binom{\nu-\frac{1}{2}}{\nu}\binom{2n-\nu-\frac{1}{2}}{2n-\nu}^2, \tag{A3}$$

and

$$V_{2(n-1),2n,2n,2n} = \frac{1}{\sqrt{2\pi}}\sum_{\nu=0}^{2(n-1)}\binom{\nu-\frac{1}{2}}{\nu}\binom{2n-\nu-\frac{1}{2}}{2n-\nu}^2\frac{(2n-\nu)(2n-\nu-1)}{\left(2n-\nu-\frac{1}{2}\right)^2}.$$

As the inequality $\frac{(2n-\nu)(2n-\nu-1)}{\left(2n-\nu-\frac{1}{2}\right)^2} < 1$ is hold, we can know that

$$\begin{aligned} V_{2(n-1),2n,2n,2n} &< \frac{1}{\sqrt{2\pi}}\sum_{\nu=0}^{2(n-1)}\binom{\nu-\frac{1}{2}}{\nu}\binom{2n-\nu-\frac{1}{2}}{2n-\nu}^2, \\ &= V_{2n,2n,2n,2n} - \frac{1}{\sqrt{2\pi}}\sum_{\nu=2n-1}^{2n}\binom{\nu-\frac{1}{2}}{\nu}\binom{2n-\nu-\frac{1}{2}}{2n-\nu}^2, \end{aligned} \tag{A4}$$

as well as

$$\begin{aligned} V_{2(n+1),2n,2n,2n} &= \frac{1}{\sqrt{2\pi}}\sum_{\nu=1}^{2n}\binom{\nu-\frac{1}{2}}{\nu}\binom{2n-\nu-\frac{1}{2}}{2n-\nu}^2\frac{2}{2\nu-1}\frac{\left(2n-\nu+\frac{1}{2}\right)^2}{(2n-\nu+1)(2n-\nu+2)}, \\ &< \frac{1}{\sqrt{2\pi}}\left[\sum_{\nu=1}^{2}\binom{\nu-\frac{1}{2}}{\nu}\binom{2n-\nu-\frac{1}{2}}{2n-\nu}^2\frac{2}{2\nu-1}\frac{\left(2n-\nu+\frac{1}{2}\right)^2}{(2n-\nu+1)(2n-\nu+2)}\right. \\ &\left. + \frac{1}{2}\sum_{\nu=3}^{2n}\binom{\nu-\frac{1}{2}}{\nu}\binom{2n-\nu-\frac{1}{2}}{2n-\nu}^2\right]. \end{aligned} \tag{A5}$$

Moreover, as the inequality $\frac{\left(2n-\nu+\frac{1}{2}\right)^2}{(2n-\nu+1)(2n-\nu+2)} < 1$ is also hold, we can have

$$\begin{aligned} &\sum_{\nu=1}^{2}\binom{\nu-\frac{1}{2}}{\nu}\binom{2n-\nu-\frac{1}{2}}{2n-\nu}^2\frac{2}{2\nu-1}\frac{\left(2n-\nu+\frac{1}{2}\right)^2}{(2n-\nu+1)(2n-\nu+2)} \\ &= \pi^{3/2}\left[\frac{(4n-5)!!}{2^{2n}(2n)!}\right]^2\left[\frac{2n(4n-1)^2(4n-3)^2}{2n+1} + \frac{4n(2n-1)^2(4n-3)^2}{2n-1}\right], \\ &< \pi^{3/2}\left[\frac{(4n-5)!!}{2^{2n}(2n)!}\right]^2\left[(4n-1)^2(4n-3)^2 + 3(2n-1)^2(4n-3)^2\right], \\ &= \pi^{3/2}\left[\frac{(4n-5)!!}{2^{2n}(2n)!}\right]^2(448n^4 - 992n^3 + 796n^2 - 276n + 36). \end{aligned} \tag{A6}$$

Then, with the fact that

$$\sum_{\nu=0}^{2}\binom{\nu-\frac{1}{2}}{\nu}\binom{2n-\nu-\frac{1}{2}}{2n-\nu}^2 = \pi^{3/2}\left[\frac{(4n-5)!!}{2^{2n}(2n)!}\right]^2[576n^4 - 896n^3 + 472n^2 - 96n + 9], \tag{A7}$$

from equations (A6) and (A7), one can reach at the following inequality:

$$\sum_{\nu=1}^{2}\binom{\nu-\frac{1}{2}}{\nu}\binom{2n-\nu-\frac{1}{2}}{2n-\nu}^2\frac{2}{2\nu-1}\frac{\left(2n-\nu+\frac{1}{2}\right)^2}{(2n-\nu+1)(2n-\nu+2)} < \sum_{\nu=0}^{2}\binom{\nu-\frac{1}{2}}{\nu}\binom{2n-\nu-\frac{1}{2}}{2n-\nu}^2, \tag{A8}$$

when $n \geqslant 1$. Consequently, combining equations (A5) and (A8), we have

$$V_{2(n+1),2n,2n,2n} < \frac{1}{2}V_{2n,2n,2n,2n} + \frac{1}{2\sqrt{2\pi}}\sum_{\nu=0}^{2}\binom{\nu-\frac{1}{2}}{\nu}\binom{2n-\nu-\frac{1}{2}}{2n-\nu}^2. \tag{A9}$$

With the results obtained in equations (A1), (A4) and (A9), the inequality shown in equation (17) can be reached

$$W_{2n,2n,2n,2n} - (4n+1)V_{2n,2n,2n,2n}$$
$$< \frac{-n}{\sqrt{2\pi}} \sum_{\nu=2n-1}^{2n} \binom{\nu - \frac{1}{2}}{\nu} \binom{2n - \nu - \frac{1}{2}}{2n - \nu}^2 - \frac{n}{2\sqrt{2\pi}} \sum_{\nu=3}^{2n} \binom{\nu - \frac{1}{2}}{\nu} \binom{2n - \nu - \frac{1}{2}}{2n - \nu}^2$$
$$+ \frac{n}{2\sqrt{2\pi}} \sum_{\nu=0}^{2} \binom{\nu - \frac{1}{2}}{\nu} \binom{2n - \nu - \frac{1}{2}}{2n - \nu}^2. \tag{A10}$$

It is noted that the last two terms shown in equation (A10) is negative when $n \geqslant 2$.
This completes the proof.

ORCID iDs

Ray-Kuang Lee https://orcid.org/0000-0002-7171-7274

References

[1] Griffiths D J 2004 *Introduction to Quantum Mechanics* 2nd edn (New Jersey: Pearson Prentice Hall)
[2] Kittel C 2004 *Introduction to Solid State Physics* 8th edn (New York: Wiley)
[3] von Roos O 1983 Position-dependent effective masses in semiconductor theory *Phys. Rev.* B **27** 7547
[4] de Souza Dutra A and Almeidab C A S 2000 Exact solvability of potentials with spatially dependent effective masses *Phys. Lett.* A **275** 25–30
[5] Schmidt A G M 2006 Wave-packet revival for the Schrödinger equation with position-dependent mass *Phys. Lett.* A **353** 459–62
[6] Jha P K, Eleuch H and Rostovtsev Y V 2011 Analytical solution to position dependent mass Schrödinger equation *J. Mod. Opt.* **58** 652–6
[7] Costa Filho R N, Almeida M P, Farias G A and Andrade J S Jr. 2011 Displacement operator for quantum systems with position-dependent mass *Phys. Rev.* A **84** 050102(R)
[8] Sebawe Abdalla M and Eleuch H 2016 Exact solutions of the position-dependent-effective mass Schrödinger equation *AIP Adv.* **6** 055011
[9] Zhou X, Wang Y, Leykam D and Chong Y D 2017 Optical isolation with nonlinear topological photonics *New J. Phys.* **19** 095002
[10] Agrawal G P 2001 *Nonlinear Fiber Optics* (New York: Academic)
[11] Lin C-Y, Chang J-H, Kurizki G and Lee R-K 2020 Solitons supported by intensity-dependent dispersion *Opt. Lett.* **45** 1471
[12] Ross R M, Kevrekidis P G and Pelinovsky D E 2021 Localization in optical systems with an intensity-dependent dispersion *Quarterly of Applied Mathematics* **79** 641
[13] Whitham G B 1965 A general approach to linear and non-linear dispersive waves using a Lagrangian *J. Fluid Mech.* **22** 273–83
[14] Whitham G B 1999 *Linear and Nonlinear Waves* (New York: Wiley)
[15] Gusev V E, Lauriks W and Thoen J 1998 Dispersion of nonlinearity, nonlinear dispersion, and absorption of sound in micro-inhomogeneous materials *J. Acous. Soc. Am.* **103** 3216
[16] Koser A A, Sen P K and Sen P 2009 Effect of intensity dependent higher-order dispersion on femtosecond pulse propagation in quantum well waveguides *J. Mod. Opt.* **56** 1812
[17] Javan A and Kelley A 1966 6A5-Possibility of self-focusing due to intensity dependent anomalous dispersion *IEEE J. Quant. Electron.* **QE-2** 470
[18] Greentree A D, Richards D, Vaccaro J A, Durrant A V, de Echaniz S R, Segal D M and Marangos J P 2003 Intensity-dependent dispersion under conditions of electromagnetically induced transparency in coherently prepared multistate atoms *Phys. Rev.* A **67** 023818
[19] Shahmoon E, Grisins P, Stimming H P, Mazets I and Kurizki G 2016 Highly nonlocal optical nonlinearities in atoms trapped near a waveguide *Optica* **3** 725–33
[20] Tsiboulia A B 2003 Gradient Index (GRIN) Lenses *Encyclopedia of Optical Engineering* ed R G Driggers vol 1 (New York: Marcel Dekker) 675–83
[21] Kunze M, Küpper T, Mezentsev V K, Shapiro E G and Turitsyn S 1999 Nonlinear solitary waves with Gaussian tails *Physica* D **128** 273
[22] Marklund M, Shukla P K, Bingham R and Mendonca J T 2006 Statistical properties of the continuum Salerno model *Phys. Rev.* A **74** 045801
[23] Gomez-Gardeñes J, Malomed B A, Floría L M and Bishop A R 2006 Solitons in the Salerno model with competing nonlinearities *Phys. Rev.* E **73** 036608
[24] Gómez-Gardeñes J, Malomed B A, Floría L M and Bishop A R 2006 Discrete solitons and vortices in the two-dimensional Salerno model with competing nonlinearities *Phys. Rev.* E **74** 036607
[25] Arfken G B and Weber H J 2005 *Mathematical Methods for Physicists* 6th edn (Boston: Elsevier Academic Press) Ch 13
[26] Pelinovsky D E and Kevrekidis P G 2007 Periodic oscillations of dark solitons in parabolic potentials *Contemp. Math.*, **473** 159
[27] D'Agosta R, Malomed B A and Presilla C 2000 Stationary solutions of the Gross-Pitaevskii equation with linear counterpart *Phys. Lett.* A **275** 424
[28] D'Agosta R, Malomed B A and Presilla C 2002 Stationary states of bose einstein condensates in single- and multi-well trapping potentials *Laser Phys.* **12** 37
[29] Gradshteyn I S and Ryzhik I M 2007 *Table of Integrals, Series, and Products* 7th edn (New York: Academic) translated from Russian by Scripta Technica
[30] Olver P J 1993 *Applications of Lie Groups to Differential Equations* 2nd edn (Berlin: Springer)
[31] Kivshar Yu S, Alexander T J and Turitsyn S K 2001 Nonlinear modes of a macroscopic quantum oscillator *Phys. Lett.* A **278** 225

[32] Praxmeyer L, Yang P and Lee R-K 2016 Phase-space representation of a non-Hermitian system with $\mathcal{PT}$ symmetry *Phys. Rev.* A **93** 042122
[33] Maimistov A I, Basharov A M, Elyutin S O and Sklyarov Y M 1990 Present state of self-induced transparency theory *Phys. Rep.* **191** 18
[34] Blaauboer M, Malomed B A and Kurizki G 2000 Spatiotemporally localized multidimensional solitons in self-induced transparency media *Phys. Rev. Lett.* **84** 1906
[35] Kozhekin A and Kurizki G 1995 Self-induced transparency in bragg reflectors: gap solitons near absorption resonances *Phys. Rev. Lett.* **74** 5020
[36] Kozhekin A E, Kurizki G and Malomed B 1998 Standing and moving gap solitons in resonantly absorbing gratings *Phys. Rev. Lett.* **81** 3647
[37] Friedler I, Petrosyan D, Fleischhauer M and Kurizki G 2005 Long-range interactions and entanglement of slow single-photon pulses *Phys. Rev.* A **72** 043803
[38] Shahmoon E, Kurizki G, Fleischhauer M and Petrosyan D 2011 Strongly interacting photons in hollow-core waveguides *Phys. Rev.* A **83** 033806